

# Characterization of focal liver lesions: Use of mangafodipir trisodium (MnDPDP)-enhanced MR images

Fokal karaciğer lezyonlarının karakterizasyonunda mangafodipir trisodyum (MnDPDP) kontrastlı MRG

Aydın KARABACAKOĞLU<sup>1</sup>, Yüksel ADIGÜZEL<sup>1</sup>, Serdar KARAKÖSE<sup>1</sup>, Ertuğrul KAYAÇETİN<sup>2</sup>, Rahime HAYKIR<sup>1</sup>

Departments of <sup>1</sup>Radiology, <sup>2</sup>Gastroenterology, Selçuk University, Meram Medical Faculty, Konya

**Background/aims:** We evaluated the characterization and detection of liver lesions using mangafodipir trisodium. **Methods:** A total of 51 patients with liver lesions [13 hepatocellular carcinomas, 18 metastases, 14 hemangiomas, three cholangiocellular carcinomas, two hydatid cysts, and one focal nodular hyperplasia (FNH)] were examined by unenhanced and mangafodipir trisodium -enhanced MRI. **Results:** After administration of mangafodipir trisodium by slow intravenous infusion, mangafodipir trisodium -enhanced MRI was performed at 15-30 min and 24 h. The enhancement appeared in normal liver parenchyma and all of the hepatocellular lesions (HCCs and FNH). The lesions in hepatocellular carcinomas patients showed a non-homogeneous enhancement pattern. Non-hepatocellular lesions (hemangiomas, metastases, CCCs) had no enhancement on mangafodipir trisodium -enhanced MRI examinations. The rim-like enhancement pattern was demonstrated in all patients with cholangiocellular carcinomas, and in 14 metastases and 11 hemangiomas. **Conclusions:** Mangafodipir trisodium -enhanced MRI permits reliable distinction between hepatocellular and non-hepatocellular tumors. Mangafodipir trisodium -enhanced MRI can show more functional and morphologic features of hepatocellular lesions. Some non-hepatocellular lesions which went undetected on unenhanced MRI were visualized after contrast enhancement of the liver. The rim-like enhancement pattern is not specific for metastases. Mangafodipir trisodium -enhanced MRI is safe and well tolerated and may aid in noninvasive diagnosis of liver lesions.

**Key words:** Mangafodipir trisodium, MRI, liver

**Amaç:** Karaciğer lezyonlarının saptanması ve karakterizasyonunda mangafodipir trisodyum kullanımının etkinliğini değerlendirmek. **Yöntem:** Karaciğerde lezyonu olan 51 hasta [13 hepatoselüler karsinom, 18 metastaz, 14 hemanjiom, 3 kolanji-oselüler karsinom, 2 kist hidatik ve 1 fokal nodüler hiperplazi] kontrastsız ve mangafodipir trisodyum kontrastlı MRG ile incelendi. **Bulgular:** Yavaş intravenöz infüzyonla mangafodipir trisodyum sonrası MRG incelemeleri infüzyondan 15-30 dk ve 24 saat sonra yapıldı. Kontrastlanma tüm hepatoselüler lezyonlarda (hepatoselüler karsinom ve fokal nodüler hiperplazi) ve normal karaciğer parankiminde görüldü. Hepatoselüler karsinomlu hastaların lezyonlarında inhomojen kontrastlanma paterni görüldü. Nonhepatoselüler lezyonlarda (hemanjiom, metastaz, kolanji-oselüler karsinom) mangafodipir trisodyum kontrastlı MRG incelemede kontrastlanma olmadı. kolanji-oselüler karsinomlu tüm hastalarda, 14 metastaz ve 11 hemanjiomlu hastada rim benzeri kontrastlanma paterni saptandı. **Sonuç:** Mangafodipir trisodyum kontrastlı MRG, hepatoselüler ve nonhepatoselüler tümörlerin güvenli bir şekilde ayırt edilmesine olanak sağlar. mangafodipir trisodyum kontrastlı MRG hepatoselüler lezyonların fonksiyonları ve morfolojik durumlarını gösterebilir. Bazı nonhepatoselüler lezyonlar kontrastsız MRG ile tanımlanamaz iken, kontrastlı incelemede vizüalze edilebilirler. Rim tarzı kontrastlanma metastazlar için spesifik değildir. mangafodipir trisodyum kontrastlı MRG güvenilir ve iyi tolere edilir, karaciğer lezyonlarının noninvasiv tanısında yardımcı olabilecek bir inceleme yöntemidir.

**Anahtar kelimeler:** Mangafodipir trisodyum, MRG, karaciğer

## INTRODUCTION

In the management of focal liver tumors, the goals (cure, palliation) and therapeutic options (surgery, chemotherapy, or radiation) are chosen based on a variety of clinical data, including the number of lesions, their size and location, their tissue type, and the number of involved liver segments (1).

The characterization of liver lesions as benign or malignant is important for the correct triage of patients to surgical versus nonsurgical therapies. Although ultrasonography (US) will depict most of the focal liver lesions, characterization of the nature often depends on additional noninvasive

**Address for correspondence:** Aydın KARABACAKOĞLU  
Department of Radiology, Selçuk University, Meram Medical Faculty,  
42080, Konya, Turkey  
Phone: +90 332 223 70 52 • Fax: +90 332 223 61 84  
E-mail: radaydin@hotmail.com

**Manuscript received:** 21.05.2005 **Accepted:** 20.02.2006

diagnostic imaging techniques such as computed tomography (CT) and magnetic resonance imaging (MRI), sometimes followed by a histopathologic examination. Dynamic contrast-enhanced CT is the most frequently used imaging modality, but it may miss hepatic lesions in a significant number of cases (2). MRI is generally reserved as a secondary diagnostic tool to characterize lesions detected on CT. Results of studies comparing lesion characteristics using these two modalities are inconclusive, mainly due to difficulty in maintaining the comparability of these two modalities in the study design. CT and MRI have a relatively narrow window of time in which an optimal image can be obtained before the distribution of contrast into the lesion interstitium obscures the lesion, because the CT and MRI contrast agents used are extracellular with no inherent organ or tissue selectivity (3-5). Thus, there is a clinical need for the development of a liver-specific contrast agent that has an extended window of time for imaging, and one that would improve focal liver lesion detection and characterization.

Liver-specific contrast agents for MRI have recently been developed and have the potential to improve the detection of focal liver lesions (6, 7). Two kinds of contrast agents have been developed for liver MRI: superparamagnetic iron oxide contrast agents, such as ferumoxides and SHU 555 A, and hepatobiliary contrast agents. The first superparamagnetic iron oxide contrast agent licensed for use was ferumoxides. Ferumoxides particles coated with dextran administered intravenously are cleared by phagocytosis of the reticuloendothelial system, including the Kupffer's cells of the liver, and predominantly shorten the T<sub>2</sub> of the liver parenchyma (8, 9). Hepatobiliary contrast agents are taken up by hepatocytes and are eliminated through the biliary system. Teslascan (MnDPDP, Amersham, GE Health Care) has a special affinity for hepatocytes and thus represents such a liver-specific MRI contrast agent. Following intravenous administration, the MnDPDP chelate dissociates slowly, and the manganese is taken up by the hepatocytes. This leads to an increase in signal intensity of normal liver parenchyma on the T<sub>1</sub>-weighted image caused by T<sub>1</sub> shortening and, thereby, to an increase in contrast between normal and abnormal tissue (10, 11).

The purposes of this study were to compare the characteristics of MnDPDP enhancement of liver lesions, and to assess whether this contrast agent

can improve differentiation between cellular composition of these lesions.

## MATERIALS AND METHODS

A total of 51 patients with liver lesions were examined by unenhanced and MnDPDP-enhanced MRI. Our patients consisted of 22 women and 29 men with a median age of 56.8 years (age range 20-76 years). The patients had a variety of conditions and findings on either US or CT and were known or suspected to have focal liver lesion. Informed consent was obtained from each patient before entry into the study. Excluded were patients who had received any contrast agent within one hour before or within 24 hours after the MnDPDP-enhanced MRI examination; who had obstructive hepatobiliary disease or biliary stasis or severe renal impairment; who were clinically unstable; for whom CT or MRI examination would be contraindicated; who had been previously enrolled into this study; or who were defined as pregnancy or lactation.

All US examinations were performed by two staff radiologists using high-resolution US equipment (Sonoline Adora, Simens, Germany) with a curvilinear 3.5 MHz transducer. All patients underwent spiral CT examination before MR examinations. For spiral CT (PQS, Picker, USA), after an initial scout, scan images (120 kV, 200-250 mA, 8 mm contiguous intervals) were acquired before administration of contrast material. Afterward, a total of 100 ml iodinated contrast agent was administered intravenously, and scans were obtained during the arterial and portal phases.

The MR examinations were performed on a 1.5-T unit (MR Edge, Picker, USA), using a body coil. Unenhanced axial fast-spin-echo T<sub>2</sub>-weighted (TR/TE: 6512/96, 192x256 matrix, 5-mm slice thickness, 1-mm gap, 90° flip angle, 50-55 cm field of view), axial and coronal spin-echo (SE) T<sub>1</sub>-weighted (TR/TE: 143/10 ms, 160x256 matrix, 5-mm slice thickness, 1-mm gap, 90° flip angle, 50-55 cm field of view, 15-20 s breath-hold), and axial and coronal T<sub>1</sub>-weighted gradient-recalled-echo (GRE) sequences (TR/TE: 155/8.1 ms, 160x256 matrix, 5-mm slice thickness, 1-mm gap, 60° flip angle, 50-55 cm field of view, 15-20 s breath-hold) were performed in all patients. MnDPDP was injected intravenously (5 µmol/kg) by slow intravenous infusion (2-3 ml/min) over a period of 15 min; MnDPDP-enhanced MRI was then performed at 15-30 min and 24 h after administration of the contrast

agent with the same protocol and sequences, except for T2-weighted fast-SE sequence, as described previously.

The MRI images were assessed by two staff radiologists. Each radiologist recorded the lesion number, lesion size, appearance of the lesion, signal intensity relative to the liver, degree of enhancement, and presence of rim-like enhancement. The conclusions were made by consensus. All imaging studies, together with histopathologic and surgical reports, were available for this review.

Each patient was monitored for adverse events, injection-associated discomfort, and changes in vital signs after administration of the liver-specific contrast agent.

## RESULTS

For each patient, baseline medical history, physical examination, vital signs, and laboratory data were obtained. In 51 patients the individual final diagnoses were as follows: 18 metastases (primary tumor: pancreatic carcinoma  $n=6$ , breast carcinoma  $n=2$ , gallbladder carcinoma  $n=1$ , leiomyosarcoma  $n=1$ , bronchial carcinoma  $n=1$ , adenocarcinoma of unknown primary site  $n=7$ ), 14 hemangiomas, 13 hepatocellular carcinomas (HCCs), three cholangiocellular carcinomas (CCCs), two hydatid cysts, and one focal nodular hyperplasia (FNH).

In three of 13 patients with HCC, two of 14 patients with hemangiomas, and one of three patients with CCC, the diagnoses were confirmed by histological examinations of tissue specimens obtained at surgery. Percutaneous needle biopsy was performed in all patients with metastases, 10 patients with HCC, two patients with CCC, and one patient with FNH. Twelve patients with hemangiomas and two patients with hydatid diseases were diagnosed based on the typical radiologic features and clinical follow-up over at least six months.

The normal liver parenchyma showed a homogeneous pattern of enhancement following administration of MnDPDP.

Six of 13 patients with HCCs had multiple HCCs with an unresectable distribution (Figure 1). Four of the remaining seven patients were positive for hepatitis B surface antigen. In these four patients, liver parenchyma showed a non-homogeneous pattern of enhancement after injection of the contrast agent. On pre-contrast images, all HCCs appeared hyperintense with a non-homogeneous internal structure in the T2-weighted sequences, while

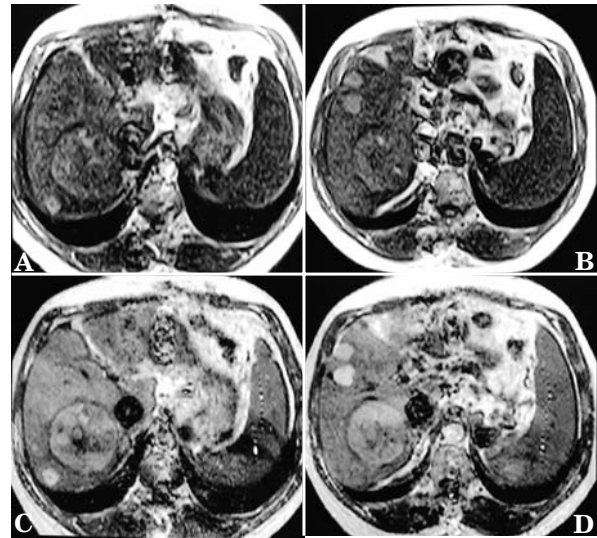


**Figure 1.** A 45-year-old man with multinodular HCC in the right lobe **A-B**) Note the different signal intensity of the different tumor nodules on unenhanced axial T1-weighted SE images, **C-D**) Same MR sequence and levels following MnDPDP infusion. The large central node shows hyperintense to the surrounding liver and the smaller nodules show hypointense peritumoral capsules. The large central node appears hyperintense with a non-homogeneous enhancement

they appeared hypo-, iso- to hyperintense in the SE and GRE T1-weighted sequences. A capsule was hypointense on both pre- and post-contrast SE and GRE T1-weighted images in nine patients with HCC. Following administration of MnDPDP, all lesions in 13 patients with HCCs showed a patchy non-homogeneous enhancement, and appeared hyperintense on both T1-weighted SE and T1-weighted GRE images (Figure 2). On the 24-h

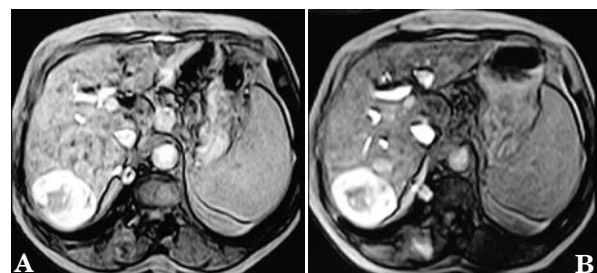


**Figure 2.** A 57-year-old man with HCC in the right lobe **A**) On MnDPDP-enhanced axial T1-weighted GRE image, the tumor shows hyperintense with a non-homogeneous enhancement. Peritumoral capsule appears hypointense on post-contrast MRI; the liver parenchyma is non-homogeneously enhanced **B**) Same MR sequence and level on delayed image (24 h post infusion). The tumor shows markedly hyperintense to the surrounding liver. Delayed image also revealed a satellite nodule

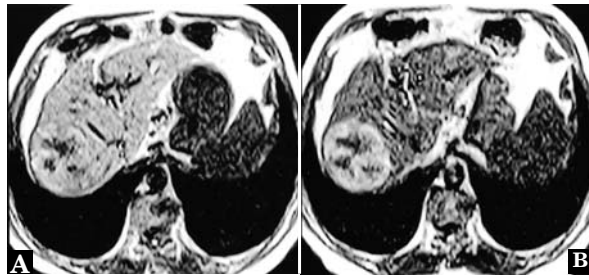


**Figure 3.** A 72-year-old man with HCC in the right lobe **A**) MnDPDP-enhanced axial T1-weighted SE image shows lesion as isointense to surrounding liver. The lesion appears as a non-homogeneous enhancement **B**) Same MR sequence and level on delayed image (24 h post infusion). The tumor shows markedly hyperintense to the surrounding liver

images, these lesions were markedly hyperintense to the surrounding liver parenchyma (Figure 3).

In one patient with FNH, central scar was seen on either pre- or post-contrast images. On unenhanced MRI images, the lesion appeared hypointense in the T1-weighted SE sequence, and showed isointense in T1-weighted GRE sequence. After MnDPDP injection at 15-30 min and 24 h, the lesion appeared hyperintense with a homogeneous internal structure on T1-weighted SE and T1-weighted GRE images. This lesion was hyperintense to the surrounding liver parenchyma after contrast injection. On 15-30 min and 24 h MnDPDP-enhanced MRI images, no enhancement of the central scar with stellate shape was depicted. No capsule was seen around of the lesion on either pre- or post-contrast images (Figure 4).

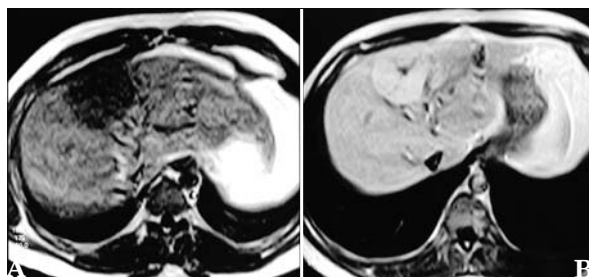


**Figure 4.** A 20-year-old man with FNH in the right lobe **A**) Unenhanced axial T1-weighted SE image shows lesion as hypointense to surrounding liver **B**) Same MR sequence and level following MnDPDP infusion. The tumor shows hyperintense to the surrounding liver with a homogeneous enhancement. Post-contrast image shows central scar without uptake of contrast agent. Note that central scar is better depicted on this image than on A

Seventeen of 18 patients with metastases had multiple lesions, and the remaining one patient had one lesion. Some of the multiple lesions were not detected on US, CT or unenhanced MRI. These metastatic lesions were visualized after contrast enhancement of the liver. All of the metastatic lesions with no enhancement on the MnDPDP-enhanced MRI examinations were identified as non-hepatocellular lesions. However, the MnDPDP-enhanced MRI images demonstrated some hyperintense ring- or rim-like zones at the periphery of the tumor, with varying degrees of enhancement in 14 patients with metastatic tumors (Figure 5).

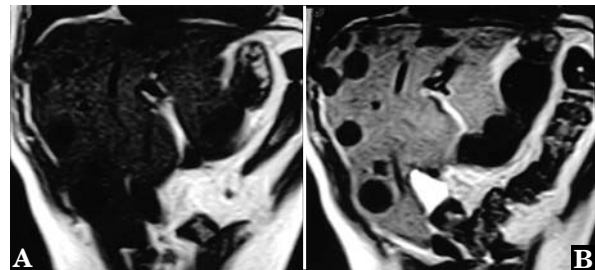


**Figure 5.** A 75-year-old man with metastatic bronchial carcinoma **A**) Unenhanced coronal T1-weighted SE image shows lesions as hypointense to surrounding liver **B**) Same MR sequence and level following MnDPDP infusion. This image clearly depicts the lesions, and demonstrates rim-like enhancement at the periphery of the lesions but no enhancement within the lesion. Also note that the normal liver parenchyma is homogeneously enhanced

Two of three patients with CCCs had one lesion, and the remaining one patient also had liver metastases (Figure 6). All of the CCCs with no enhancement on the MnDPDP-enhanced MRI examinations were identified as non-hepatocellular lesion. However, the MnDPDP-enhanced MRI images demonstrated some hyperintense ring- or rim-like zones at the periphery of the tumor, with varying degrees of enhancement in all patients with CCC.

In 14 patients with hemangiomas and two patients with hydatid cyst, hemangiomas and cysts presented a smoother, round-to-lobular appearance, and were markedly hyperintense in the T2-weighted image, while they appeared hypointense in the T1-weighted sequences both before and after administration of MnDPDP. All of the hydatid cysts and hemangiomas with no enhancement on

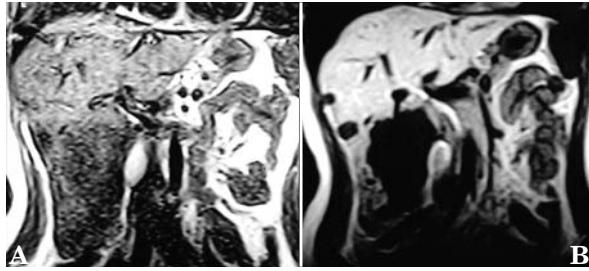


**Figure 6.** A 36-year-old woman with CCC and metastatic lesions **A**) Unenhanced coronal T1-weighted SE image shows suspicious lesions as hypointense to surrounding liver **B**) Same MR sequence and level following MnDPDP infusion. The normal liver parenchyma enhances brightly, making CCC lesions more evident because of no enhancement within the lesion. More metastases and greater conspicuousness of lesions are noted

the MnDPDP-enhanced MRI examinations were identified as non-hepatocellular lesion. However, the MnDPDP-enhanced MRI images demonstrated some hyperintense ring- or rim-like zones at the periphery of the tumor, with varying degrees of enhancement in 11 patients with hemangioma (Figure 7).

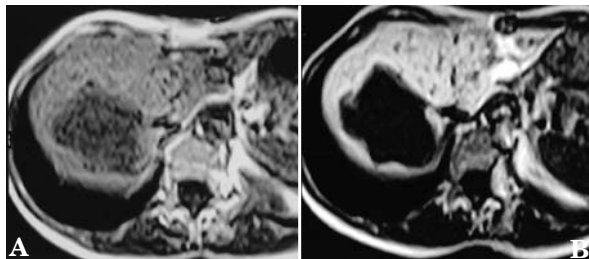


**Figure 7.** A 48-year-old woman with hemangioma in the right lobe **A**) Unenhanced axial T1-weighted SE image shows ill-defined and lobular appearance of large lesion as hypointense to surrounding liver **B**) Same MR sequence and level following MnDPDP infusion. This image shows rim-like enhancement at the periphery of the lesion but no enhancement within the lesion

The MnDPDP-enhanced MRI exams provided additional diagnostic information that was not provided by all other available clinical and imaging methods. The signal intensity of FNH and HCCs was significantly improved on the MnDPDP-enhanced T1-weighted SE and T1-weighted GRE images at 15-30 min and 24 h compared with pre-contrast images. In 14 of 51 patients, enhancement of the lesions could be observed after MnDPDP administration. MnDPDP-enhanced MRI images showed an advantage for differenti-

ating hepatocellular lesions (HCC, FNH) from non-hepatocellular lesions (metastasis, CCC, hemangioma, and hydatid cyst).

There was no correlation between non-hepatocellular lesion type and pattern of rim-like enhancement.

Tolerance of Teslascan was good. No patient experienced adverse reactions, injection-associated discomfort or change in vital signs.

## DISCUSSION

Magnetic resonance imaging provides useful strategies for detection and characterization of liver tumors. However, because of wide biologic variability and considerable overlap in the T1 and T2 relaxation times of tumor and normal liver, many lesions exhibit only a subtle change in intensity compared with normal liver tissue or they are isointense (12, 13). MnDPDP is a T1-shortening paramagnetic contrast agent that causes enhancement of normal liver tissues. However, MnDPDP offers the additional advantages of a longer retention by the liver and hence a longer window of time for imaging (5). In healthy livers, parenchymal enhancement can be observed early after the injection and up to 24 h later. Near maximal enhancement of the normal liver parenchyma is obtained 15-20 min from start of administration and lasts for approximately 4 h (14). In our study, MnDPDP was injected intravenously by slow intravenous infusion over a period of 15 min; MnDPDP-enhanced MRI was then performed at 15-30 min and 24 h after administration of the contrast agent with the SE and GRE T1-weighted sequences.

Cirrhosis is a common clinical setting for HCC, and the similar imaging appearance of benign and malignant hepatocellular nodules is troublesome. Features that may suggest HCC, including heterogeneous enhancement or the presence of a peritumoral capsule, will be helpful in differentiation (15). Murakami *et al.* demonstrated that the enhancement in cirrhotic liver parenchyma was significantly less than that in noncirrhotic liver parenchyma, 15 min after injection of MnDPDP. This early lesser enhancement could be due to decreased uptake of MnDPDP because of liver dysfunction or fibrotic changes (16). In our study, there was lower enhancement of the liver parenchyma in chronic hepatitis and an entirely heterogeneous pattern was observed.

MnDPDP shows uptake only in liver lesions such as HCC, FNH, and hepatocellular adenoma, which are composed of functional hepatocytes (17, 18). Recently presented data suggest that delayed imaging might be more useful for detecting and differentiating hepatic lesions than imaging performed directly after contrast administration (10, 17). Because the rate of elimination of MnDPDP from the hepatocytes has been shown to be strongly delayed in the presence of biliary obstruction, retention of MnDPDP within HCC could be attributed to the absence of functional biliary system, or to obstruction of intratumoral bile ducts either by tumoral casts or by compression (17, 19).

In our study, signal intensity of HCC remained high in comparison with signal intensity of the surrounding liver parenchyma, denoting retention of MnDPDP within HCC on delayed 24 h images. Capsules surrounding HCCs did not enhance on post-contrast images, even on delayed 24 h images. On pathology, these capsules were made of fibrotic tissue. This lack of enhancement improves the contrast between the tumor and the surrounding liver parenchyma, outlining the presence of an eventual capsule (15).

Morphologic features in FNH that have some degree of tissue specificity include tumor homogeneity, iso- to hypointensity on T1-weighted MRI, iso- to hyperintensity on T2-weighted MRI, and the presence of central scar that is hyperintense on T2-weighted MRI (18). In a study by Coffin et al., the signal intensity of the FNH was higher than that of the surrounding normal liver parenchyma on MRI obtained after MnDPDP infusion. This difference in intensity may seem surprising because both liver and FNH consist of normal hepatocytes, but it can be explained by a higher rate of contrast uptake or a lower rate of elimination of the contrast agent in FNH lesions compared with normal liver, or a combination of both (17).

In our study, tumoral enhancement after MnDPDP injection distinguished between HCCs and FNH due to the better detection of morphologic patterns, such as a central scar in a lesion or peripheral capsule or homogeneity. Following administration of MnDPDP, the lesions showed a patchy non-homogeneous enhancement in all patients, and also peritumoral capsules were depicted in nine patients with HCCs. FNH lesion appeared hyperintense with a homogeneous internal structure on post-contrast images. This lesion was hyperintense to the surrounding liver parenchyma

after contrast injection. No detection of a peritumoral capsule and better visualization of central scar allowed a more confident diagnosis.

MnDPDP consistently produces bright enhancement of normal liver due to a T1-shortening effect. Thus MnDPDP-enhanced MRI is most likely simply the increased image contrast between normal liver parenchyma and non-hepatocellular lesion. The improved performance of MnDPDP-enhanced MRI compared with contrast-enhanced CT may be related not only to a more tissue-specific contrast effect because of cellular uptake of MnDPDP (whereas iodinated agents are extracellular in distribution), but also to the stability of the MnDPDP enhancement over time relative to the rapidly changing contrast effects seen during contrast-enhanced CT (5). Helmberger et al. (20) reported that no significant contrast-to-noise ratio changes were seen in hemangiomas after bolus injection of MnDPDP. This might indicate that in relatively early scanning, the expected contrast-to-noise ratio change in hemangiomas is compensated by the combined effects of still-intravascular contrast together with contrast transported into the hepatocytes of the surrounding tissue. In our study, all of the metastatic lesions, CCCs, hydatid cysts, and hemangiomas having no enhancement on the MnDPDP-enhanced MRI examinations at 15-30 min and 24 h after administration of the contrast agent were identified as non-hepatocellular lesion. Although some of multiple lesions were not detected on US, CT or unenhanced MRI, these metastatic lesions are visualized after contrast enhancement (MnDPDP) of the liver.

The rim-like enhancement on MnDPDP-enhanced MRI has been seen in metastases originating from colon carcinomas. The underlying mechanism for the occurrence of rim-like enhancement in some metastatic liver tumors has been attributed to several causes. First, peritumoral malignant infiltration into neighboring normal liver parenchyma can result in intermingling of non-hepatocellular malignant cells with normal hepatocytes in the peripheral region of liver metastasis. Second, compression of surrounding normal liver tissue by a metastatic tumor mass may lead to impaired MnDPDP excretion or persistent MnDPDP retention because of the compressed bile canaliculi in these areas (19, 21, 22). Kane et al. (19) reported such a rim-like enhancement phenomenon in a patient with CCC, which is known to infiltrate neighboring normal liver tissue. In our study,

rimlike enhancement 1on MnDPDP-enhanced MRI was demonstrated in all patients with CCC, in 14 metastases, and in 11 hemangiomas. The rim-like enhancement is usually observed in metastatic malignant tumors, but rim-like enhancement pattern is not specific or pathognomonic.

Serious adverse events with MnDPDP-enhanced MRI are rare and are not contrast-related. The most commonly reported adverse events are nausea and headache (10, 23, 24). The injection-associated discomforts of heat and flushing are most common with higher injection rates and are probably related to peripheral vasodilatation (10, 23). In our study, tolerance of MnDPDP was good. No patient experienced adverse reactions, injection-associated discomfort or change in vital signs after slow intravenous infusion over a period of 15 min.

In conclusion, MnDPDP-enhanced MRI permits

reliable distinction between hepatocellular and non-hepatocellular tumors. MnDPDP-enhanced MRI can show more functional and morphologic features of hepatocellular lesions, and is helpful in differentiating between FNH and HCC. Some non-hepatocellular lesions which were not detected on unenhanced MRI are visualized after contrast enhancement of the liver. The rim-like enhancement demonstrates in patients with non-hepatocellular lesion such as metastasis, CCC, and hemangioma. Thus, rim-like enhancement pattern is not specific for metastases.

MnDPDP-enhanced MRI can be reserved as a diagnostic tool (before turning to invasive procedures) when the diagnosis is inconclusive by other imaging findings, combined with clinical information. MnDPDP-enhanced MRI is safe and well tolerated and may aid in noninvasive diagnosis of liver lesions.

## REFERENCES

- Seltzer SE, Holman BL. Imaging hepatic metastases from colorectal carcinoma: identification of candidates for partial hepatectomy. *AJR* 1989; 152: 917-23.
- Heiken JP, Weyman PJ, Lee JK, et al. Detection of focal hepatic masses: prospective evaluation with CT, delayed CT, CT during arterial portography, and MR imaging. *Radiology* 1989; 171: 47-51.
- Heiken JP, Brink JA, McClellan BL, et al. Dynamic contrast-enhanced CT of the liver: comparison of contrast medium injection rates and uniphasic and biphasic injection protocols. *Radiology* 1993; 187: 327-31.
- Runge VM, Pels Rijcken TH, Davidoff A, et al. Contrast-enhanced MR imaging of the liver. *J Magn Reson Imaging* 1994; 4: 281-9.
- Federle M, Chezmar J, Rubin DL, et al. Efficacy and safety of mangafodipir trisodium (MnDPDP) injection for hepatic MRI in adults: results of the U.S. multicenter phase III clinical trials. Efficacy of early imaging. *J Magn Reson Imaging* 2000; 12: 689-701.
- Bluemke DA, Paulson EK, Choti MA, et al. Detection of hepatic lesions in candidates for surgery: comparison of ferumoxides-enhanced MR imaging and dual-phase helical CT. *AJR* 2000; 175: 1653-8.
- Ward J, Naik KS, Guthrie JA, et al. Hepatic lesion detection: comparison of MR imaging after the administration of superparamagnetic iron oxide with dual-phase CT by using alternative-free response receiver operating characteristic analysis. *Radiology* 1999; 210: 459-66.
- Stark DD, Weissleder R, Elizondo G, et al. Superparamagnetic iron oxide: clinical application as a contrast agent for MR imaging of the liver. *Radiology* 1988; 168: 297-301.
- Ros PR, Freeny PC, Harms SE, et al. Hepatic MR imaging with ferumoxides: a multicenter clinical trial of the safety and efficacy in the detection of focal hepatic lesions. *Radiology* 1995; 196: 481-8.
- Torres CG, Lundby B, Sterud AT, et al. MnDPDP for MR imaging of the liver: results from the European phase III studies. *Acta Radiol* 1997; 38: 631-7.
- Liou J, Lee JK, Borrello JA, Brown JJ. Differentiation of hepatomas from nonhepatomatous masses: use of MnDPDP-enhanced MR images. *Magn Reson Imaging* 1994; 12: 71-9.
- Semelka RC, Shoenut JP, Kroeker MA, et al. Focal liver disease: comparison of dynamic contrast enhanced CT and T2-weighted fat-suppressed, FLASH, and dynamic gadolinium-enhanced MR imaging at 1.5 T. *Radiology* 1992; 184: 687-94.
- Marti-Bonmati L, Masia L, Torrijo C, et al. Dynamic MR imaging of liver tumors: analysis with temporal reconstruction images. *Radiology* 1994; 193: 677-82.
- Wang C, Gordon PB, Hustvedt SO, et al. MR imaging properties and pharmacokinetics of MnDPDP in healthy volunteers. *Acta Radiol* 1997; 38: 665-76.
- Murakami T, Baron RL, Peterson MS, et al. Hepatocellular carcinoma: MR imaging with mangafodipir trisodium (MnDPDP). *Radiology* 1996; 200: 69-77.
- Murakami T, Baron RL, Federle MP, et al. Cirrhosis of the liver: MR imaging with mangafodipir trisodium (MnDPDP). *Radiology* 1996; 198: 567-72.
- Coffin CM, Diche T, Mahfouz A, et al. Benign and malignant hepatocellular tumors: evaluation of tumoral enhancement after mangafodipir trisodium injection on MR imaging. *Eur Radiol* 1999; 9: 444-9.
- Ba-Ssalamah A, Schima W, Schmook MT, et al. Atypical focal nodular hyperplasia of the liver: imaging features of nonspecific and liver-specific MR contrast agents. *AJR* 2002; 179: 1447-56.
- Kane PA, Ayton V, Walters HL, et al. MnDPDP-enhanced MR imaging of the liver: correlation with surgical findings. *Acta Radiol* 1997; 38: 650-4.
- Helmberger TK, Laubenberger J, Rummeny E, et al. MRI characteristic in focal hepatic disease before and after administration of MnDPDP: discriminant analysis as a diagnostic tool. *Eur Radiol* 2002; 12: 62-70.
- Ni Y, Marchal G, Yu J, et al. Experimental liver cancers: MnDPDP-enhanced rims in MR-microangiographic-histologic correlation study. *Radiology* 1993; 188: 45-51.

22. Oudkerk M, Torres CG, Song B, et al. Characterization of liver lesions with mangafodipir trisodium-enhanced MR imaging: multicenter study comparing MR and dual-phase spiral CT. *Radiology* 2002; 223: 517-24.
23. Federle MP, Chezmar JL, Rubin DL, et al. Safety and efficacy of mangafodipir trisodium (MnDPDP) injection for hepatic MRI in adults: results of the U.S. multicenter phase III clinical trials (safety). *J Magn Reson Imaging* 2000; 12: 186-97.
24. Marti-Bonmati L, Fog AF, de Beeck BO, et al. Safety and efficacy of mangafodipir trisodium in patients with liver lesions and cirrhosis. *Eur Radiol* 2003; 13: 1685-92.